

## Chiral Phosphine–Phosphite Ligands in the Highly Enantioselective Rhodium-Catalyzed Asymmetric Hydrogenation

Sirik Deerenberg,<sup>†</sup> Oscar Pàmies,<sup>‡</sup> Montserrat Diéguez,<sup>‡</sup> Carmen Claver,<sup>\*,‡</sup>  
Paul C. J. Kamer,<sup>†</sup> and Piet W. N. M. van Leeuwen<sup>\*,†</sup>

*Institute of Molecular Chemistry, Universiteit van Amsterdam, Nieuwe Achtergracht 166,  
1018 WV Amsterdam, The Netherlands, and Department de Química Física i Inorgànica,  
Universitat Rovira i Virgili, Pl. Imperial Tarraco 1, 43005 Tarragona, Spain*

claver@quimica.urv.es

Received April 24, 2001

We have investigated a series of enantiopure phosphine–phosphite ligands ( $P_1$ – $P_2$  = ligands **1**–**4**) in the rhodium-catalyzed asymmetric hydrogenation reaction. Intermediate  $[Rh(P_1$ – $P_2)(cod)]BF_4$  and  $[Rh(P_1$ – $P_2)(5)]BF_4$  complexes (cod = 1,5-cyclooctadiene; **5** = methyl acetamidoacrylate ester) were observed by  $^{31}P\{^1H\}$  NMR. The  $[Rh(P_1$ – $P_2)(cod)]BF_4$  complexes were precursors to active catalysts of the asymmetric hydrogenation reaction of several prochiral dehydroamino acid derivatives under mild reaction conditions (1 bar of hydrogen and 20 °C). The enantiomeric excess reached up to 99%.

### Introduction

Over the years, the scope for the asymmetric hydrogenation of alkenes has gradually extended, both in reactant structure and catalyst efficiency.<sup>1</sup> Phosphorus ligands are among the most widely used chiral ligands in this process.<sup>1</sup> Most of them are derivatives of aryl- or alkylidiphosphines. In the past few years, a group of less electron-rich phosphorus compounds—phosphite ligands—have demonstrated their potential utility in asymmetric hydrogenation.<sup>2</sup> Bearing in mind Achiwa's idea that two different donor sites can a priori lead to a better match of the intermediates determining reactivity and enantioselectivity,<sup>3,4</sup> we recently described the first application of phosphine–phosphite ligands in hydrogenation (Figure 1).<sup>5</sup> The combination of both types of functionalities was beneficial for enantiodiscrimination. Phosphine–phosphite with xylofuranoside backbone ligands therefore resulted in better enantioselectivities than their diphosphine<sup>6</sup> and diphosphite<sup>2b</sup> analogues.

Despite the early success of DIPAMP in asymmetric hydrogenation,<sup>7</sup> considerably less attention has been paid to ligand structures bearing asymmetrically substituted

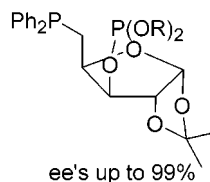


Figure 1.

phosphorus donors. In this respect, van Leeuwen et al. recently designed a new class of chiral phosphine–phosphite ligands (**1**–**4**) with a stereogenic phosphine that have the advantages of both types of ligand (Figure 2).<sup>8</sup> In this paper, we describe how this series of optically pure phosphine–phosphite ligands **1**–**4** (Figure 2) affects the rate and enantioselectivity of the asymmetric hydrogenation reaction of methyl (*N*)-acetylaminocinnamate and methyl (*Z*)-(*N*)-acetylaminocinnamate. The advantage of these ligands is that many structural variations can be made that can provide information about how the different stereocenters affect enantioselectivity. This study may provide some insight into the origin of the stereochemistry of the reaction.<sup>8</sup> We investigated the effect of the stereogenic phosphine moiety by introducing different substituents into the phosphorus atom. We also studied the influence of the group attached to the stereogenic carbon next to the phosphite moiety and the size of the substituent and examined ligands containing a shorter linker, thus enforcing a smaller P–Rh–P angle. Finally, we discuss intermediate rhodium complexes under hydrogenation conditions and conduct kinetic studies to get more insight in the mechanism of the asymmetric hydrogenation reaction.

<sup>†</sup> Universiteit van Amsterdam.

<sup>‡</sup> Universitat Rovira i Virgili.

(1) (a) Noyori, R. *Asymmetric Catalysis in Organic Synthesis*; Wiley: New York, 1994. (b) *Catalytic Asymmetric Synthesis*; Ojima, I., Ed.; Wiley: New York, 2000. (c) *Comprehensive Asymmetric Catalysis*; Jacobsen, E. N.; Pfaltz, A.; Yamamoto, H., Eds.; Springer, Berlin, 1999; vol. 1.

(2) (a) Reetz, M. T.; Neugebauer, T. *Angew. Chem., Int. Ed.* **1999**, *38*, 179. (b) Pàmies, O.; Net, G.; Ruiz, A.; Claver, C. *Eur. J. Inorg. Chem.* **2000**, 1287. (c) Reetz, M. T.; Mehler, G. *Angew. Chem., Int. Ed.* **2000**, *39*, 3889.

(3) Inoguchi, K.; Sakuraba, S.; Achiwa, K. *Synlett* **1992**, 169.

(4) For some successful applications of this idea, see for instance: (a) Nozaki, K.; Sakai, N.; Nanno, T.; Higashijima, T.; Mano, S.; Horiuchi, T.; Takaya, H. *J. Am. Chem. Soc.* **1997**, *119*, 4413. (b) Knöbel, A. K. H.; Escher, I. J.; Pfaltz, A. *Synlett* **1997**, 1429. (c) Prétôt, R.; Pfaltz, A. *Angew. Chem., Int. Ed.* **1998**, *37*, 323. (d) Hu, X.; Chen, H.; Zhang, X. *Angew. Chem., Int. Ed.* **1999**, *38*, 3518.

(5) Pàmies, O.; Diéguez, M.; Net, G.; Ruiz, A.; Claver, C. *Chem. Commun.* **2000**, 2383.

(6) Pàmies, O.; Net, G.; Ruiz, A.; Claver, C. *Eur. J. Inorg. Chem.* **2000**, 2011.

(7) (a) Knowles, W. S.; Sabacky, M. J.; Vineyard, B. D. *J. Chem. Soc., Chem. Commun.* **1972**, 10. (b) Brunner H.; Zettlmeier, W. *Handbook of Enantioselective Catalysis*; VCH: Weinheim, 1993.

(8) (a) Deerenberg, S.; Kamer, P. C. J.; van Leeuwen, P. W. N. M. *Organometallics* **2000**, *19*, 2065. (b) Deerenberg, S.; Schrekker, H. S.; van Strijdonck, G. P. F.; Kamer, P. C. J.; van Leeuwen, P. W. N. M.; Fraanje, J.; Goubitz, K. *J. Org. Chem.* **2000**, *65*, 4810. (c) Diéguez, M.; Deerenberg, S.; Claver, C.; van Leeuwen, P. W. N. M.; Kamer, P. C. J. *Tetrahedron: Asymmetry* **2000**, *11*, 3161.

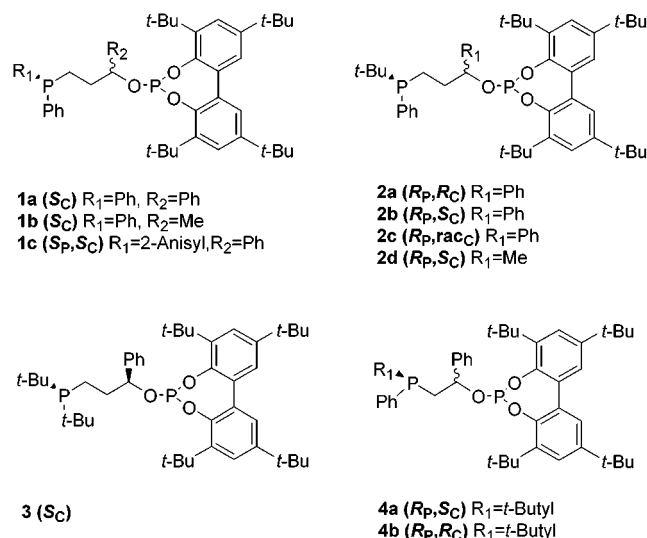


Figure 2.

## Results and Discussion

**Ligands Design.** Phosphine–phosphite ligands consist of a phosphine group and a phosphite moiety with a bulky atropisomerically chiral tetra(*tert*-butyl)bisphenol group.<sup>8a,b</sup> The donor atoms are connected by a linker that contains a stereogenic carbon. The phosphine moieties of ligands **1a** and **1b** contain two phenyl substituents, whereas ligand **1c** has an *o*-anisyl and a phenyl substituent and contains a stereogenic phosphorus atom. The stereocenter at the backbone contains a phenyl group for ligands **1a** and **1c** and a methyl group for ligand **1b**. The electronic character is expected to be similar for ligands **1** so we can investigate how the influence of the substituent of the backbone affects the enantioselectivity.

Ligands **2** are more electron donating due to the *tert*-butyl group, and they have a stereogenic P-atom. We investigated the influence of the stereogenic phosphorus atom by comparing diastereomeric ligands **2a**, **2b**, and **2c**, which is a 1:1 mixture of epimers of opposite configuration at the bridge stereocenter and *R*-configured phosphine moiety. Ligand **2d** contains the smaller methyl substituent at the stereogenic carbon.

The two *tert*-butyl substituents of the phosphine moiety make ligand **3** even more electron donating and more bulky than ligands **2** and reduce its  $\pi$ -electron-accepting properties.

Ligands **4a** and **4b** resemble ligands **2a** and **2b**, respectively, but have a shorter backbone, thus enforcing a smaller P–Rh–P angle. The orientation of the substituents at the carbon stereocenter is similar despite the absolute configuration<sup>9</sup> of the carbon stereocenters.

**Synthesis of the Alkene Complexes.** The reaction of chiral phosphine–phosphite ligands (**1–4**) with  $[\text{Rh}(\text{cod})_2]\text{BF}_4$  in a dichloromethane solution proceeded readily to provide high yields of  $[\text{Rh}(\text{P}_1\text{–P}_2)(\text{cod})]\text{BF}_4$  ( $\text{P}_1 =$  phosphite,  $\text{P}_2 =$  phosphine) cationic complexes (Scheme 1).

### Scheme 1



**Table 1.**  $^{31}\text{P}\{^1\text{H}\}$  NMR Data for Complexes  $[\text{Rh}(\text{P}_1\text{–P}_2)(\text{cod})]\text{BF}_4$  ( $\text{P}_1\text{–P}_2 = \mathbf{1}\text{–}\mathbf{3}$ )<sup>a,b</sup>

ligand	$\text{P}_1 =$ phosphite		$\text{P}_2 =$ phosphine		
	$\delta(\text{P}_1)$	$J\{\text{P}_1\text{–Rh}\}$	$\delta(\text{P}_2)$	$J\{\text{P}_2\text{–Rh}\}$	$J\{\text{P}_1\text{–P}_2\}$
<b>1a</b>	130.9	263.1	29.6	149.5	42.7
<b>1b</b>	126.5	269.2	29.4	132.3	42.9
<b>1c</b>	130.5	262.3	30.9	139.5	42.9
<b>2a</b>	130.0	260.5	36.0	133.2	40.6
<b>2b</b>	130.3	261.2	35.9	133.5	40.9
<b>2c</b>	130.1	259.8	35.6	133.7	40.7
<b>2d</b>	129.8	261.2	31.4	132.6	43.8
<b>3</b>	129.9	260.8	34.8	130.4	40.1

<sup>a</sup> Chemical shifts ( $\delta$ ) in ppm, coupling constants ( $J$ ) in hertz.

<sup>b</sup> The spectra were recorded at room temperature.

**Table 2.**  $^{31}\text{P}\{^1\text{H}\}$  NMR Data for Complexes  $[\text{Rh}(\text{P}_1\text{–P}_2)(\text{cod})]\text{BF}_4$  ( $\text{P}_1\text{–P}_2 = \mathbf{4a}$  and  $\mathbf{4b}$ )<sup>a</sup>

ligand	$\text{P}_1 =$ phosphite		$\text{P}_2 =$ phosphine		
	$\delta(\text{P}_1)$	$J\{\text{P}_1\text{–Rh}\}$	$\delta(\text{P}_2)$	$J\{\text{P}_2\text{–Rh}\}$	$J\{\text{P}_1\text{–P}_2\}$
<b>4a</b>	124.1	248.4	21.0	140.2	54.4
<b>4a</b> (65%) <sup>b</sup>	122.4	248.6	22.1	141.2	52.3
<b>4a</b> (35%) <sup>b</sup>	127.3	248.9	18.5	140.1	55.3
<b>4b</b>	127.3	249.7	20.0	136.8	53.5
<b>4b</b> (55%) <sup>b</sup>	126.1	251.3	15.1	132.2	53.1
<b>4b</b> (45%) <sup>b</sup>	128.3	250.2	23.8	138.9	54.1

<sup>a</sup> Chemical shifts ( $\delta$ ) in ppm, coupling constants ( $J$ ) in hertz.

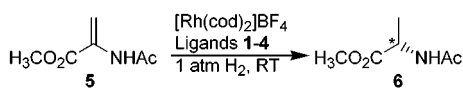
<sup>b</sup>  $T = 213$  K. Relative abundance between brackets.

At 293 K the  $^{31}\text{P}\{^1\text{H}\}$  NMR spectra for complexes  $[\text{Rh}(\text{P}_1\text{–P}_2)(\text{cod})]\text{BF}_4$  ( $\text{P}_1\text{–P}_2 = \mathbf{1}\text{–}\mathbf{3}$ ) (Table 1) showed a sharp double doublet in the phosphite region due to the  $J\{\text{P}_1\text{–P}_2\}$  and  $J\{\text{P}_1\text{–Rh}\}$  couplings, while in the phosphine region a broad doublet was obtained ( $\Delta\omega_{1/2} \approx 40$  Hz). This suggests fluxional processes on the NMR time-scale, which was confirmed by low temperature  $^{31}\text{P}\{^1\text{H}\}$  NMR spectroscopy. At 193 K the  $^{31}\text{P}\{^1\text{H}\}$  NMR spectra showed sharp double doublets in the phosphine and in the phosphite region, which indicates that only one complex was present.

At room temperature,  $^{31}\text{P}\{^1\text{H}\}$  NMR spectra for complexes  $[\text{Rh}(\text{P}_1\text{–P}_2)(\text{cod})]\text{BF}_4$  ( $\text{P}_1\text{–P}_2 = \mathbf{4a}$  and  $\mathbf{4b}$ ) (Table 2) showed two sharp double doublets. When the temperature was lowered, there were two sets of signals in different proportions (Table 2).

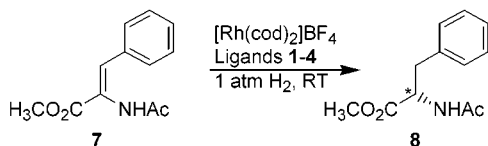
These results are consistent with the presence of two isomeric forms (**a** and **b**) in fast exchange on the NMR time-scale at room temperature. The formation of different isomers may be caused by two diastereoisomers obtained from the atropisomerism of the bisphenol in the phosphite moiety, different conformers for the six-membered chelate ring or a combination of the two. Although the rapid ring inversion of the seven-membered dioxaphosphenin rings has been detected on the NMR time-scale in the free ligands,<sup>8a,b</sup> we expect the bisphenol moiety to be in one configuration in the related cationic complexes  $[\text{Rh}(\text{P}_1\text{–P}_2)(\text{cod})]\text{BF}_4$ , as with other complexes.<sup>2b,8a,b,10</sup> This suggests the presence of different conformers of the six-membered chelate ring.

**Asymmetric Hydrogenation Results.** We tested the catalytic performance of the complexes with the phosphine–phosphite ligands in the enantioselective rhodium-catalyzed hydrogenation reactions of methyl (*N*)-acetyl-aminoacrylate **5** and methyl (*Z*)-(*N*)-acetylaminocinnamate

**Table 3. Asymmetric Hydrogenation of Methyl (*N*-Acetylaminoacrylate<sup>a</sup>**

entry	ligands	solvent	TOF <sup>b</sup>	conv [%] (h) <sup>c</sup>	ee [%] (config) <sup>d</sup>
1	( <i>S</i> <sub>C</sub> )- <b>1a</b>	MeOH	30.1	97 (4)	93 ( <i>R</i> )
2	( <i>S</i> <sub>C</sub> )- <b>1a</b>	THF	22	84 (4)	94 ( <i>R</i> )
3	( <i>S</i> <sub>C</sub> )- <b>1a</b>	CH <sub>2</sub> Cl <sub>2</sub> /MeOH <sup>e</sup>	9.2	78 (14)	98 ( <i>R</i> )
4	( <i>S</i> <sub>C</sub> )- <b>1a</b>	CH <sub>2</sub> Cl <sub>2</sub>	7.4	77 (14)	99 ( <i>R</i> )
5	( <i>S</i> <sub>C</sub> )- <b>1b</b>	CH <sub>2</sub> Cl <sub>2</sub>	18.1	39 (2.5)	96 ( <i>S</i> )
6	( <i>S</i> <sub>P</sub> , <i>S</i> <sub>C</sub> )- <b>1c</b>	CH <sub>2</sub> Cl <sub>2</sub>	12.3	100 (14)	4 ( <i>S</i> )
7	( <i>R</i> <sub>P</sub> , <i>R</i> <sub>C</sub> )- <b>2a</b>	CH <sub>2</sub> Cl <sub>2</sub>	42.2	100 (2.5)	96 ( <i>S</i> )
8	( <i>R</i> <sub>P</sub> , <i>S</i> <sub>C</sub> )- <b>2b</b>	CH <sub>2</sub> Cl <sub>2</sub>	41.3	100 (2.5)	95 ( <i>R</i> )
9	( <i>R</i> <sub>P</sub> )- <b>2c</b>	CH <sub>2</sub> Cl <sub>2</sub>	41.2	100 (2.5)	6 ( <i>R</i> )
10	( <i>R</i> <sub>P</sub> , <i>S</i> <sub>C</sub> )- <b>2d</b>	CH <sub>2</sub> Cl <sub>2</sub>	52.1	100 (2.5)	95 ( <i>S</i> )
11	( <i>S</i> <sub>C</sub> )- <b>3</b>	CH <sub>2</sub> Cl <sub>2</sub>	4.8	21 (5)	58 ( <i>R</i> )
12	( <i>R</i> <sub>P</sub> , <i>S</i> <sub>C</sub> )- <b>4a</b>	CH <sub>2</sub> Cl <sub>2</sub>	19.1	32 (2.5)	61 ( <i>S</i> )
13	( <i>R</i> <sub>P</sub> , <i>R</i> <sub>C</sub> )- <b>4b</b>	CH <sub>2</sub> Cl <sub>2</sub>	225 <sup>f</sup>	100 (1)	96 ( <i>R</i> )

<sup>a</sup> All reactions were run at ambient temperature under 1 bar of H<sub>2</sub>. Cinnamate-to-rhodium ratio is 100. Ligand-to-rhodium ratio is 1.1. <sup>b</sup> After 1 h [in mol·mol<sup>-1</sup>·h<sup>-1</sup>]. <sup>c</sup> Percentage conversion of cinnamate determined by GC. <sup>d</sup> Enantiomeric excess determined by GC. Absolute configuration drawn in parentheses. <sup>e</sup> Ratio 9/1. <sup>f</sup> Determined after 10 min.

**Table 4. Asymmetric Hydrogenation of Methyl (*Z*)-(*N*-Acetylaminocinnamate<sup>a</sup>**

entry	ligands	TOF <sup>b</sup>	conv [%] (h) <sup>c</sup>	ee [%] (config) <sup>d</sup>
14	( <i>S</i> <sub>C</sub> )- <b>1a</b>	6.2	100 (24)	97 ( <i>R</i> )
15	( <i>S</i> <sub>C</sub> )- <b>1b</b>	14	100 (24)	92 ( <i>S</i> )
16	( <i>S</i> <sub>P</sub> , <i>S</i> <sub>C</sub> )- <b>1c</b> <sup>e</sup>	9	100 (24)	6 ( <i>S</i> )
17	( <i>R</i> <sub>P</sub> , <i>R</i> <sub>C</sub> )- <b>2a</b>	34.8	100 (12)	95 ( <i>S</i> )
18	( <i>R</i> <sub>P</sub> , <i>S</i> <sub>C</sub> )- <b>2b</b>	35	100 (12)	95 ( <i>R</i> )
19	( <i>R</i> <sub>P</sub> )- <b>2c</b> <sup>e</sup>	33.9	100 (12)	3 ( <i>R</i> )
20	( <i>R</i> <sub>P</sub> , <i>S</i> <sub>C</sub> )- <b>2d</b> <sup>e</sup>	44.3	100 (12)	89 ( <i>S</i> )
21	( <i>S</i> <sub>C</sub> )- <b>3</b>	3.9	85 (24)	63 ( <i>R</i> )
22	( <i>R</i> <sub>P</sub> , <i>S</i> <sub>C</sub> )- <b>4a</b> <sup>e</sup>	9.6	100 (12)	65 ( <i>S</i> )
23	( <i>R</i> <sub>P</sub> , <i>R</i> <sub>C</sub> )- <b>4b</b> <sup>e</sup>	100	100 (1)	95 ( <i>R</i> )

<sup>a</sup> All reactions were run at ambient temperature under 1 bar of H<sub>2</sub>. Cinnamate-to-rhodium ratio is 100. Ligand-to-rhodium ratio is 1.1. <sup>b</sup> After 1 h [in mol·mol<sup>-1</sup>·h<sup>-1</sup>]. <sup>c</sup> Percentage conversion of cinnamate determined by GC. <sup>d</sup> Enantiomeric excess determined by GC. Absolute configuration drawn in parentheses. <sup>e</sup> Substrate/rhodium = 1/50.

**7** under 1 bar of H<sub>2</sub>. The catalyst was formed in situ from [Rh(cod)<sub>2</sub>]BF<sub>4</sub> and 1.1 equivalent of the ligands **1**–**4**. The results of this study are shown in Tables 3 and 4. For both methyl (*N*-acetylaminoacrylate **5** and methyl (*Z*)-(*N*-acetylaminocinnamate **7**, high enantioselectivities were achieved up to 99% and 97%, respectively. Products other than (*N*-acetylalanine methyl ester **6** and (*N*-acetylphenylalanine methyl ester **8** were not observed. In general, the hydrogenation of methyl (*N*-acetylaminoacrylate **5** was somewhat faster than that of methyl (*Z*)-(*N*-acetylaminocinnamate **7**.

The hydrogenation of methyl (*N*-acetylaminoacrylate was performed in several solvents. Rhodium-catalyzed asymmetric hydrogenation reactions are commonly performed in methanol. For the reaction in methanol using **1a** a high enantioselectivity of 93% and a high rate were

observed (entry 1). The reaction in tetrahydrofuran showed similar ee, but the rate was lower (entry 2). For reactions performed in dichloromethane/methanol (9/1) and pure dichloromethane, the enantiomeric excess increased to 98% and 99%, respectively (entries 3 and 4). However, the reaction rate decreased and the highest ee corresponded to the slowest reaction. Since phosphite ligands are known to decompose in protic solvents,<sup>11</sup> further hydrogenation reactions were studied using dichloromethane.

The hydrogenation reaction performed with ligand **1a**, which contains a phenyl substituent at the stereocenter of the backbone, produced the *R*-enantiomer in 99% ee. Ligand **1b**, which has a methyl substituent in a different spatial arrangement than the phenyl, afforded the *S*-configured product in 96% ee (entry 5). The changed configuration of the products indicated that enantioselectivity was mainly controlled by the configuration of the substituent in the backbone.<sup>9</sup> The ee decreased slightly due to the smaller methyl group of ligand **1b**, but the reaction rate is improved. When we used ligand **1c**, which contains a phosphine moiety with an anisyl substituent, the ee was low (entry 6). Since the substituents of the phosphorus and carbon stereocenters are similarly oriented for ligand **1c** and **1a**, we concluded that the anisyl group was responsible for the decrease in rate and enantioselectivity.

For ligands **2**, which contain a strongly electron-donating stereogenic phosphine, the reaction rate was higher than that for ligands **1**. In the hydrogenation reaction complexes containing ligands, **2a** and **2b** afforded similar ee's of 96% (*S*) and 95% (*R*), respectively (entries 7 and 8). Since the ligands only differ in configuration of the stereocenter in the backbone, this indicates that the stereogenic phosphine moiety does not influence enantioselectivity. We therefore concluded that enantioselectivity was predominantly controlled by the stereocenter of the backbone. This was confirmed by the experiment using ligand **2c**, which is the mixture of **2a** and **2b**, and for which a low ee of 6% was obtained (entry 9). Ligand **2d**, which has a small methyl substituent at the bridge, gave a higher reaction rate than **1b**, which contains a phenyl substituent (entry 10). The ee obtained with **2d** was similar to that obtained when ligand **2a** was applied.

Ligand **3**, which contains a more basic and bulky phosphine moiety than ligands **1** and **2**, produced moderate ee's of 58% and a relatively low reaction rate in the hydrogenation (entry 11). This indicates that both reaction rate and enantioselectivity may be influenced by the steric hindrance of the bulky *tert*-butyl groups at the phosphine moiety in the interaction with the alkene. The greater steric hindrance may slow the oxidative addition of dihydrogen, which requires rotation of substrate versus ligand.<sup>12</sup>

Using ligand **4b**, which has a shorter linker between the phosphine and the phosphite moieties, we observed the highest reaction rate of all ligands used and an ee of 96% (entry 13). Diastereomer **4a** produced a lower ee of 61% and a lower reaction rate (entry 12). The difference

(11) a) Baker, M. J.; Harrison, K. N.; Orpen, A. G.; Shaw, G.; Pringle, P. G. *J. Chem. Soc., Chem. Commun.* **1991**, 803. (b) Nirchio, P. C.; Wink, D. J. *Organometallics* **1991**, *10*, 336.

(12) a) Feldgus, S.; Landis C. R. *J. Am. Chem. Soc.* **2000**, *122*, 12714. (b) Landis, C. R.; Feldgus, S. *Angew. Chem., Int. Ed.* **2000**, *39*, 2863 and references therein.



in reactivity and selectivity between rhodium complexes containing ligands **4a** and **4b** is remarkable when compared to ligands **2a** and **2b**, which both afforded similar ee's of different enantiomers. We suggest that the small bite angles of the rhodium complexes containing ligands **4** enhance a cooperative effect between the stereocenters, which results in a matched combination for ligand **4b** and a mismatched combination for ligand **4a**. Ligands **1–3** have a larger bite angle, and therefore the substituents of the phosphine moiety and the carbon stereocenter are not in close proximity.

Table 4 shows the results of the rhodium-catalyzed hydrogenation of methyl (*Z*)-(*N*)-acetylaminocinnamate. In general, the hydrogenation of methyl (*Z*)-(*N*)-acetylaminocinnamate followed the same trend as that of methyl (*N*)-acetyl aminoacrylate. However, the enantiomeric excesses were somewhat smaller, and the reaction rates were lower. Using the same ligand in the hydrogenation reaction of methyl (*N*)-acetyl aminoacrylate and methyl (*Z*)-(*N*)-acetylaminocinnamate produced the same configurations for the corresponding products **6** and **8**, respectively, and similar ee's. The catalyst containing ligand **1a** gave the highest ee of 97% (*R*) for this series at a low reaction rate (entry 14). Ligand **4b** afforded the highest reaction rate, and there was a cooperative effect between the stereogenic phosphine moiety and the stereocenter at the backbone (entry 23). Complexes with ligands **2** and **4** afforded the highest reaction rates together with high enantioselectivities of all the ligands used.

**Mechanistic Considerations.** The mechanism of the enantioselective hydrogenation catalyzed by cationic diphosphine rhodium complexes has been thoroughly studied. The widely accepted catalytic cycle, a result from the work by the groups of Brown, Halpern, Landis, and Bosnich, involves the reversible binding of the substrate to the catalyst, followed by the rate-determining oxidative addition of H<sub>2</sub> and the subsequent rapid elimination of the hydrogenated product.<sup>13</sup> Halpern's classic studies<sup>13a</sup> on hydrogenation have shown that enantioselectivity is determined by the ratio of the initially formed diastereoisomers of [Rh(P<sub>1</sub>–P<sub>2</sub>)(substrate)]<sup>+</sup> complexes (Figure 3) and the respective reactivities of these intermediates toward H<sub>2</sub>. Since phosphine–phosphite ligands have different properties compared to diphosphines, the catalytic sequence is not necessarily the same. To learn more about the catalytic cycle, we monitored the hydrogenation of methyl acetamidoacrylate ester (**5**) using ligand **2a** by <sup>31</sup>P{<sup>1</sup>H} NMR. We examined a solution of [Rh(**2a**)(cod)]BF<sub>4</sub> in dichloromethane-*d*<sub>2</sub> at 1 bar of dihydrogen, but a [Rh(**2a**)(cod)H<sub>2</sub>] species was not detected. After methyl acetamidoacrylate ester was added, two new double

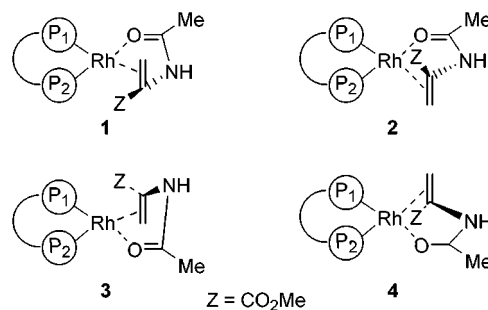


Figure 3. Diastereomeric [Rh(P<sub>1</sub>–P<sub>2</sub>)(**5**)] complexes.

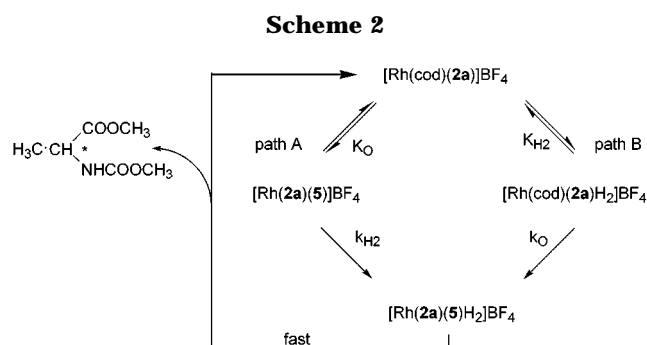


Table 5. Kinetic Data for the Hydrogenation of **5** Catalyzed by [Rh(**2a**)(cod)]BF<sub>4</sub> in Dichloromethane

P <sub>H<sub>2</sub></sub> <sup>a</sup>	[Rh( <b>2a</b> )(cod)]BF <sub>4</sub> <sup>b</sup>	TOF <sup>c</sup>
1	0.0017	42.1
2	0.0017	75.3
3	0.0017	131.7
1	0.005	117.8
1	0.0005	13.2

<sup>a</sup> Pressure in bar. <sup>b</sup> Concentration in mol·l<sup>-1</sup>. <sup>c</sup> TOF measured in mol·molRh<sup>-1</sup>·h<sup>-1</sup>.

doublets at 136.02 and 35.57 ppm were observed in the <sup>31</sup>P{<sup>1</sup>H} NMR spectrum. These new signals were assigned to the cationic rhodium complex [Rh(**2a**)(**5**)]<sup>+</sup> and attributed to the phosphine and phosphite moieties, respectively. The P<sub>1</sub>–P<sub>2</sub> coupling constant is 56 Hz, whereas *J*{P<sub>1</sub>–Rh} and *J*{P<sub>2</sub>–Rh} are 241 and 161 Hz, respectively. The shift of the phosphite signal in the <sup>31</sup>P{<sup>1</sup>H} NMR spectrum of complex [Rh(**2a**)(**5**)]BF<sub>4</sub> is consistent with a diastereoisomer the phosphite of which is *trans* to the C=O fragment and the phosphine of which is *trans* to the C=C fragment.<sup>13a</sup> Variable-temperature <sup>31</sup>P{<sup>1</sup>H} NMR spectra between 303 and 193 K showed that only one diastereoisomer was present. Furthermore, the formation of hydride species was not observed in the <sup>1</sup>H NMR spectrum.

These results show that the so-called alkene pathway (pathway A, Scheme 2) seems to be the preferred route. Pathway B (Scheme 2), in which a dihydrogen complex was formed, cannot be excluded, since species [Rh(**2a**)(cod)H<sub>2</sub>]BF<sub>4</sub> may be present in amounts below the detection limit of the NMR equipment.

To obtain more insight into the sequence of the cycle, we studied the rate dependence on substrate concentration, hydrogen pressure, and rhodium concentration. The data collected in Table 5 indicate that the reaction is first order in rhodium concentration and hydrogen pressure.

For a typical hydrogenation reaction, performed at standard conditions, the formation of hydrogenated product shows a zeroth-order dependency on substrate

(13) (a) Landis, C. R.; Halpern, J. *J. Am. Chem. Soc.* **1987**, *109*, 1746. (b) Brown, J. M.; Chaloner, P. A.; Morris, G. A. *J. Chem. Soc., Chem. Commun.* **1983**, 644. (c) Brown, J. M.; Evans, P. L. *Tetrahedron Lett.* **1988**, *44*, 4905. (d) Bodgan, P. L.; Irwin, J. J.; Bosnich, B. *Organometallics* **1989**, *8*, 1450. (e) Alcock, N. W.; Brown, J. M.; Derome, A. E.; Lucy, A. R. *J. Chem. Soc., Chem. Commun.* **1985**, 575. (f) Allen, D. G.; Wild, S. B.; Wood, D. L. *Organometallics* **1986**, *5*, 1009. (g) Brown, J. M.; Maddox, P. J. *J. Chem. Soc., Chem. Commun.* **1987**, 1278. (h) Brown, J. M.; Chaloner, P. A.; Morris, G. A. *J. Chem. Soc., Perkin Trans. 2* **1987**, 1583. (i) McCulloch, B. M.; Halpern, J. T., M. R.; Landis, C. R. *Organometallics* **1990**, *9*, 1392. (j) Brown, J. M. *Chem. Soc. Rev.* **1993**, *22*, 25. Landis, C. R.; Brauch, T. W. *Inorg. Chim. Acta* **1998**, *270*, 285. (k) Kimmich, B. F. M.; Somsook, E.; Landis, C. R. *J. Am. Chem. Soc.* **1998**, *120*, 10115. (l) Landis, C. R.; Hilfenhaus, P.; Feldgus, S. *J. Am. Chem. Soc.* **1999**, *121*, 8741. (m) RajanBabu, T. V.; Radetich, B.; You, K. K.; Ayers, T. A.; Casalnuovo, A. L.; Calabrese, J. C. *J. Org. Chem.* **1999**, *64*, 3429.

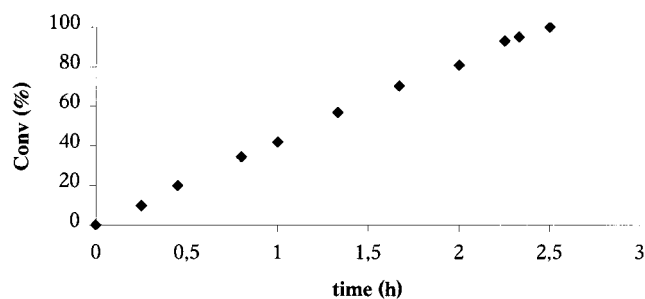


**Figure 4.** Hydrogenation of methyl (*N*)-acetylaminoacrylate.

(5) concentration (Figure 4). Our results so far suggest that the addition of hydrogen is the rate-determining step. An alternative explanation for the zeroth-order in substrate relates to the work recently reported by Heller et al. who found that the asymmetric hydrogenation of prochiral olefins takes place parallel to that of the diolefin stemming from the catalyst precursor.<sup>14</sup> We therefore performed experiments to clarify whether an incubation time related to the slow hydrogenation of cyclooctadiene could give a false zeroth-order dependency on substrate concentration. When an excess of 1 mmol of cyclooctadiene was added, the plot of conversion over time was the same as the one in Figure 4. This confirmed the zeroth-order dependency on the substrate concentration.

In summary, from these results it seems reasonable to assume that the addition of H<sub>2</sub> is the rate-determining step. This agrees with the Landis–Halpern mechanism (path A, Scheme 2). However, the evidence is not conclusive since the same rate-law would be obtained if there is a fast equilibration between [Rh(2a)(5)]BF<sub>4</sub> as the dominant species and a minor amount of [Rh(2a)(cod)-H<sub>2</sub>]<sub>2</sub>BF<sub>4</sub>, followed by a rate-determining addition of 5 to the latter complex.

**Origin of Enantioselectivity.** In the past, the enantioselectivity achieved with several known C<sub>2</sub>-symmetric diphosphine–rhodium catalysts was explained with the aid of quadrant diagrams.<sup>15</sup> However, this simple method does not explain why a reaction involving such a small dihydrogen molecule can lead to such enormous differences in rate for the diastereomeric alkene adducts present. Research by Brown, Burk, and Landis led to the “rotation mechanism” (Figure 5).<sup>12b</sup> The prochiral enamide substrate coordinates in a bidentate fashion and the square planar Rh-complex is formed. Due to steric hindrance of the ligand toward the substrate, one of the diastereomeric complexes is energetically more favored and forms in excess. The oxidative addition of dihydrogen can take place from the top or the bottom of the complex, and dihydrogen will coordinate in a *cis* fashion. The carbonyl fragment migrates together with rotation of the alkene fragment. The steric hindrance exerted by the ligand determines which diastereomeric rhodium–dihydride complex will be formed and thus leads to the enantiomeric product. For several systems it was found that the minor diastereomeric rhodium–substrate species led to the major product.<sup>13a,h,i</sup>

Using the present phosphine–phosphite ligands, the alkene coordinates *cis* toward the sterically more demanding phosphite moiety.<sup>13a</sup> Our hydrogenation experiments showed that the substituent of the stereogenic

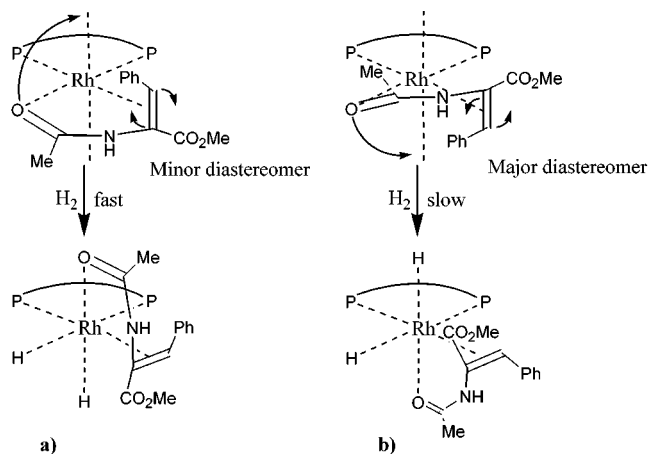


**Figure 5.** Rotation mechanism upon oxidative addition for diastereomeric intermediates a and b: Attack of H<sub>2</sub> from the bottom a or from the top b.

carbon has the strongest effect on enantioselectivity. Since the substituent of the backbone is positioned at the back of the complex, and a previous study showed that the substituent at the backbone controls the configuration of the phosphite moiety, which on its turn determines the enantioselectivity,<sup>8a–b,10</sup> we expect the bulky biphenol moiety to play a major role in determining the enantioselectivity.

## Conclusions

We investigated the rhodium-catalyzed asymmetric hydrogenation reaction of methyl (*N*)-acetylaminoacrylate and methyl (*Z*)-(*N*)-acetylaminoacrylate using a series of enantiopure phosphine–phosphite ligands (1–4). Excellent enantioselectivities of up to 99% were obtained under mild conditions. Systematically varying the steric and electronic properties of the ligands showed that enantioselectivity is determined by the stereogenic carbon in the backbone. Although the phosphine moiety does not affect enantioselectivity, an electron-donating phosphine improves the reaction rate. Studies on intermediates of the catalytic cycle of the reaction using <sup>31</sup>P{<sup>1</sup>H} NMR indicate that the [Rh(P<sub>1</sub>–P<sub>2</sub>)(5)]<sup>+</sup> species is the resting state of the reaction and that the rate dependence is first order in rhodium and hydrogen pressure and zeroth order in substrate. The alkene coordinates *trans* to the phosphine moiety, and we propose that the phosphite moiety determines the enantioselectivity of the reaction controlled by the substituent of the stereogenic carbon. For ligands 4, which enforce a smaller bite angle, there was a cooperative effect between the two stereogenic groups.

## Experimental Section

**General Considerations.** Chemicals were obtained from Acros Chimica and Aldrich. All syntheses were performed using standard Schlenck techniques under argon atmosphere. Complex [Rh(cod)<sub>2</sub>]<sub>2</sub>BF<sub>4</sub><sup>16</sup> and ligands 1–4<sup>8a–b</sup> were prepared by previously described methods. Solvents were distilled and deoxygenated before use. NMR spectra were recorded on a Varian Gemini 300 MHz spectrometer.

(14) Börner, A.; Heller, D. *Tetrahedron Lett.* **2001**, *42*, 223.

(15) Knowles, W. S. *Acc. Chem. Res.* **1983**, *16*, 106.

(16) Green, M.; Kuc, T. A.; Taylor, S. H. J. *J. Chem. Soc. A* **1971**, 2334.

**Preparation of Cationic Rhodium Complexes.** In a general procedure, phosphine–phosphite ligand (0.05 mmol) was added to a solution of  $[\text{Rh}(\text{cod})_2]\text{BF}_4$  (20.2 mg, 0.05 mmol) in dichloromethane (2 mL). After 5 min, the desired products were obtained by precipitation with hexane as orange solids in good yields (around 90%).

**In Situ NMR Characterization Experiments. (1)  $[\text{Rh}(\text{cod})(\text{P}_1\text{-P}_2)]\text{BF}_4$  under  $\text{H}_2$  Pressure. Procedure A.** Hydrogen was bubbled through a solution of  $[\text{Rh}(\text{cod})(\text{P}_1\text{-P}_2)]\text{BF}_4$  (0.015 mmol) in dichloromethane- $d_2$  (1.0 mL) at room temperature in an NMR tube. The reaction was followed by NMR.

Procedure B. In a typical experiment a sapphire tube ( $\Phi = 10$  mm) was filled under argon with a solution of  $[\text{Rh}(\text{cod})(\text{P}_1\text{-P}_2)]\text{BF}_4$  (0.02 mmol) in dichloromethane- $d_2$  (1.5 mL). The tube was purged twice and pressurized to 1.2 bar of  $\text{H}_2$ . The reaction was followed under  $\text{H}_2$  pressure.

**(2)  $[\text{Rh}(\text{cod})(\text{P}_1\text{-P}_2)]\text{BF}_4$  and Methyl Acetamidoacrylate Ester.** In a typical experiment, a sapphire tube ( $\Phi = 10$  mm) was filled under argon with a solution of  $[\text{Rh}(\text{cod})(\text{P}_1\text{-P}_2)]\text{BF}_4$  (0.02 mmol) and methyl acetamidoacrylate ester (0.1 or 0.25

mmol) in dichloromethane- $d_2$  (1.5 mL). The reaction was followed by  $^{31}\text{P}\{^1\text{H}\}$  NMR.

**Asymmetric Hydrogenation Reactions.** In a typical run a Schlenk vessel filled with a solution of substrate (1 mmol), catalyst precursor  $[\text{Rh}(\text{cod})_2]\text{BF}_4$  (0.01 mmol), and the ligand (molar ratio  $\text{P}_1\text{-P}_2/\text{Rh} = 1.1$ ) in dichloromethane (6 mL) was purged three times with  $\text{H}_2$ . The reaction mixture was then shaken under  $\text{H}_2$  (1 atm) at 298 K. After the desired reaction time, the conversion and enantioselectivity were measured by GC (fused silica capillary column 25 m  $\times$  0.25 mm permabond L-Chirasil-Val).

**Acknowledgment.** We thank the Spanish Ministerio de Educaci3n y Cultura and the Generalitat de Catalunya (CIRIT) for their financial support (PB97-04007-CO5-01). Financial support from CW/STW is also gratefully acknowledged (project no. 349-3590).

JO015705D